

Electronic Supplementary Information

A novel fluorescent aptasensor for ultrasensitive and selective detection of acetamiprid pesticide based on inner filter effect between gold nanoparticles and carbon dots

Jinlong Wang ^a, Yuangen Wu ^{a,*}, Pei Zhou ^b, Wenping Yang ^a, Han Tao ^a, Shuyi Qiu ^{a,*}, Caiwei Feng ^c

^a Guizhou Province Key Laboratory of Fermentation Engineering and Biopharmacy; School of Liquor and Food Engineering, Guizhou University, Guiyang 550025, Huaxi District, Guizhou Province, China

^b Key Laboratory of Urban Agriculture (South), Ministry of Agriculture; School of Agriculture and Biology, Shanghai Jiao Tong University, Shanghai 200240, China

^c Engineering Research Center of Nation Combined with Local on Biological Detection Technologies for Food Safety, Guizhou Kwinbon Food Safety Science and Technology Co., Ltd, Guiyang 550025, China

* Corresponding author at: School of Liquor and Food Engineering, Guizhou University, Guiyang 550025, Guizhou Province, China.

E-mail address: wuyg1357@163.com (Y. Wu), syqiu@gzu.edu.cn (S. Qiu).

Materials and methods

Quantum Yield Calculations

The quantum yield (Φ) of the carbon dots (CDs) was calculated using quinine sulfate as reference^{1,2}. Briefly, the quinine sulfate (literature $\Phi = 0.54$) was dissolved in 0.1 M H₂SO₄ (refractive index (η) of 1.33) while the CDs was dissolved in water ($\eta = 1.33$). Using quinine sulfate as a reference, the integrated fluorescence intensities and the absorbance values (less than 0.05) of the prepared CDs and quinine sulfate were measured.

The quantum yield was calculated using the below equation:

$$\Phi = \Phi_R \times \frac{I}{I_R} \times \frac{A_R}{A} \times \frac{\eta^2}{\eta_R^2}$$

Where Φ , I , η refer to the quantum yield, the measured integrated emission intensity and refractive index, respectively. A is the absorbance values and the subscript R is the reference fluorescent substance of known quantum yield. The quantum yield for the as-prepared CDs is calculated to be 64.5%.

Preparation of AuNPs

Citrate-coated AuNPs (CC-AuNPs) were obtained by classical citrate reduction of HAuCl_4 according to our previous reports³. In Briefly, 10 mL of 38.8 mM sodium citrate solution was rapidly added to a boiling 100 mL of 1.0 mM HAuCl_4 solution under vigorous stirring. The mixed solution was boiled for 15 min and further stirred for another 15 min then cooled to room temperature and filtered using an ultrafiltration membrane (250 nm aperture). In the case of cysteamine-stabilized AuNPs (CS-AuNPs), 1.2 mL of 213 mM cysteamine and 1.42 mM HAuCl_4 were mixed, and then the mixture was blended under ambient temperature for 20 min. Subsequently, 30 mL of 10 mM NaBH_4 was added to the above solution, and the mixture was stirred for another 25 min at room temperature in the dark⁴. As for unmodified AuNPs (umAuNPs), according to the borohydride reduction method, 1.5 mL of 29.43 mM HAuCl_4 solution was diluted with 118.5 mL bi-distilled water. Afterward, 3 mL of 264.34 mM NaBH_4 solution were added dropwise under vigorous stirring. The resulting wine-red colloidal solution was further stirred for 30 min and then left undisturbed overnight⁵. All the AuNPs solutions were stored in a refrigerator at 4 °C, and their amounts were determined according to Bouguer–Lambert–Beer law: $A = kcd$ (where A is the absorption, k is the molar extinction coefficient, c is the sample concentration and d is the optical path length). $c = A_{450} / \epsilon_{450}$, where c is in mol per litre and the absorption A at 450 nm for a standard path length of 1 cm is used.

The operating parameters of LC-MS

Compare with previous literature⁶, the liquid chromatography-mass spectrometry (LC-MS) analysis of acetamiprid was carried out on a Shimadzu (Tokyo, Japan) 20 AD-XR LC system (Shimadzu Corporation, Kyoto, Japan). The column was an Agilent Eclipse XDB-C18 column (4.6 mm × 150 mm, 5 μm particle size, Agilent California, USA). The LC operating parameters were as follows: the column temperature was 40 °C, and the flow rate was 0.8 mL/min with an injection volume of 5 μL. The mobile phase was a mixture of a 0.1% formic acid aqueous solution (A) and acetonitrile (B). The chromatographic gradient started at 10% B (0.0–0.5 min), increased to 95% B (0.5–7.5 min), held at 95% B (7.5–8.0 min), decreased to 10% B (8.0–8.01 min), and maintained at 10% B (8.01–10.0 min). The retention times of acetamiprid were approximately 3.64 min.

An Applied Biosystems Sciex API 4000Q Trap quadrupole mass spectrometer equipped with an Ion Source Turbo Spray unit (Thermo Fisher Scientific, Waltham, USA) was applied to quantify the acetamiprid pesticide. The curtain gas, nebulizer gas and collision gas were all nitrogen. The electrospray ionization (ESI) source-dependent parameter settings were as follows: declustering potential, 77.1 V; curtain gas pressure, 25.0 kPa; ion spray voltage, 5500 V; ion source temperature, 600 °C; ion source gas 1 pressure, 55.0 kPa; and ion source gas 2 pressure, 55.0 kPa. The analysis of acetamiprid was performed in positive mode using multiple reaction monitoring (MRM) with two mass transitions. The m/z 223.1→126.0 transition was set as the quantification transition, and the m/z 223.1→56.1 transition was set as the confirmation transition. The collision energy was set at 27 and 35 V for product ions 126.0 and 56.1, respectively.

Table S1 Comparison of fluorescent quantum yields of the previously reported carbon dots synthesized by hydrothermal method

CD	Materials	The range of size(nm)	The surface potential (mV)	Quantum yield (%)	Ref
1	Citric acid anhydrous + ethylenediamine + deionized water	2-6	-7.2	65.5	7
2	Citric acid + ethylenediamine + deionized water	2-5	-6.2	76	8
3	Aspartic acid + deionized water	3.0-4.5	-5.9	41.3	9
4	Citric acid + (NH ₄) ₂ HPO ₄ + deionized water	1.5-4	-4.8	59	10
5	Citric acid + ethylenediamine + deionized water	3-7	- 2.6	64.5	This work

Table S2 Comparison with earlier aptamers-based methods for acetamiprid detection

Methods	Transduction principle	Linear range ($\mu\text{g} \cdot \text{L}^{-1}$)	LOD ($\mu\text{g} \cdot \text{L}^{-1}$)	Ref
Colorimetry	The peroxidase activity of AuNPs is controlled by the specific binding of the target and aptamers to catalyze TMB	100-1.0 $\times 10^4$	100	11
	The enhanced peroxidase activity of AuNPs based on the specific binding of the target and aptamers to catalyze ABTS	10-50	1.02	12
	Aggregation of AuNPs based on the specific binding of the target and aptamers in NaCl solution	17-1.7 $\times 10^3$	1.1	13
Electrochemistry	Signal amplification utilizing AuNPs as the support for aptamer immobilization	56-446	19	14
	A decrease of the enhanced photocurrent produced by the electron donor of quercetin based on the specific binding of the target and aptamers	0.1-178	0.04	15
Chemiluminescence	Aggregation of AuNPs based on the high binding of the target and aptamers which amplifies the chemiluminescence signal in the presence of luminol and H_2O_2	None	0.01	16
Fluorescence	Release of the fluorescein-labeled complementary strand of the aptamer (CS) from the aptamer/CS conjugate based on the specific binding of the target and aptamers	0.09-156	0.03	17
	Aggregation of AuNPs based on the specific binding of the target and aptamers and turns on the fluorescence of CdTe QDs	11-223	1.6	18
	Reduce the fluorescence intensity of probe based on the dissociation of cDNA-UCNPs from aptamer-MNPs through the specific binding of the target and aptamers	0.89-114.18	0.65	19
	Release fluorescent signal from the internal filter effect quenching of dispersed AuNPs toward CDs based on the specific binding of the target and aptamers	5-100	1.08	This work

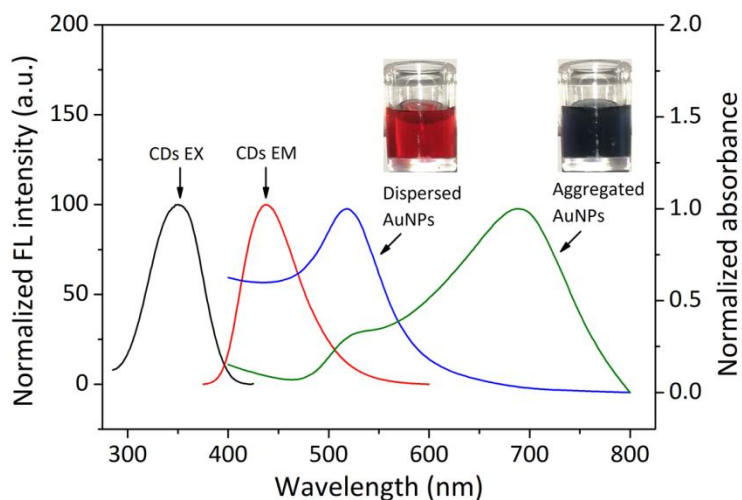


Fig. S1 Normalized excitation and emission spectra of CDs integrated with the color and normalized absorption spectra of dispersed and aggregated CC-AuNPs

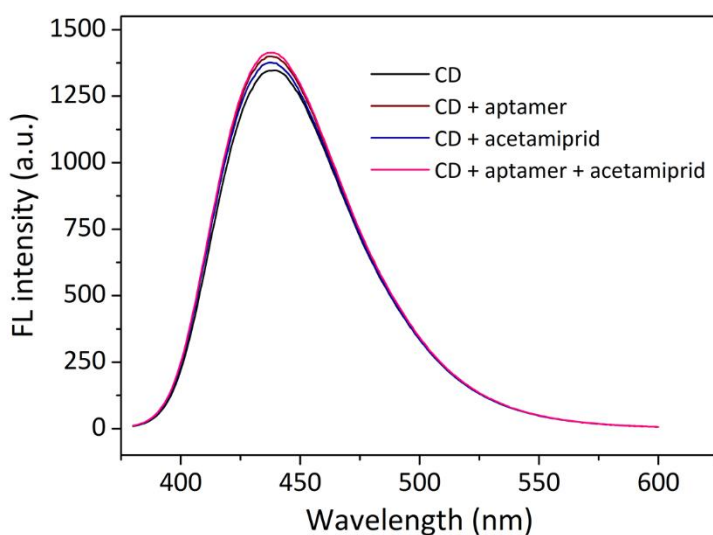


Fig. S2 Emission spectra of the prepared CDs treated with S-18 aptamer or acetamiprid. The concentrations of CDs, acetamiprid and S-18 aptamer were $0.2 \text{ mg}\cdot\text{mL}^{-1}$, $1 \text{ mg}\cdot\text{L}^{-1}$ and 25 nM , respectively. The excitation and emission wavelength were 350 nm and 437 nm .

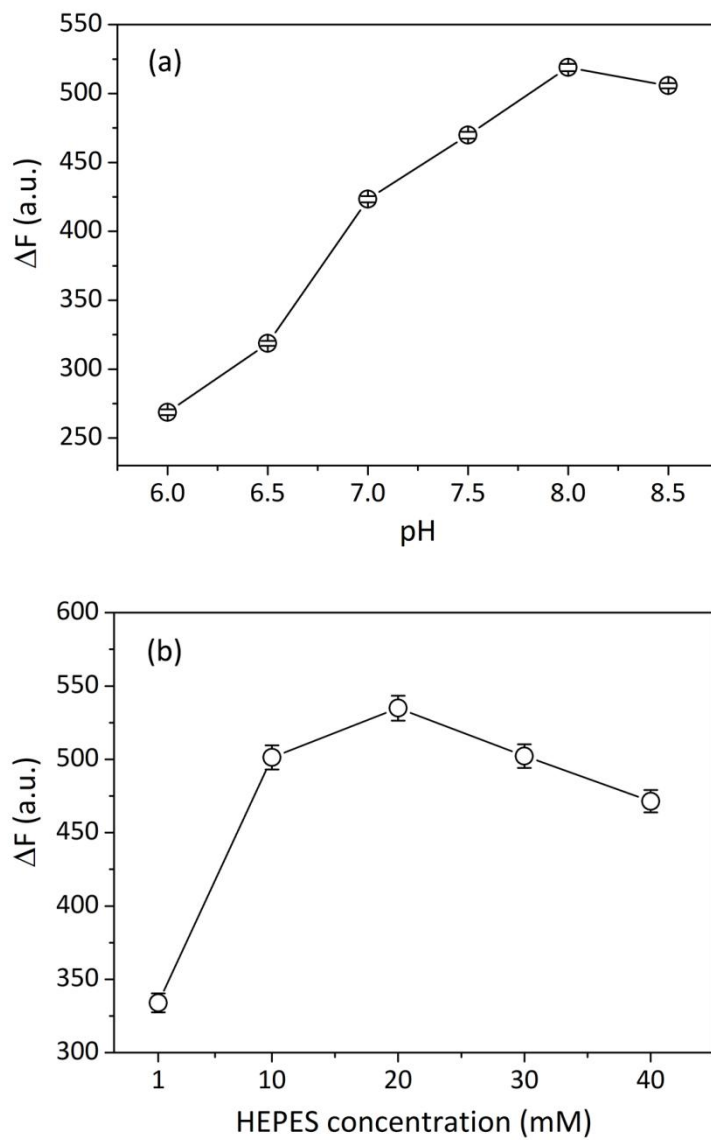


Fig. S3 Effect of pH (a) and HEPES concentration (b) on the aptasensor. The concentrations of CDs, CC-AuNPs and S-18 aptamer were $0.2 \text{ mg}\cdot\text{mL}^{-1}$, 3.2 nM and 25 nM , respectively. The excitation and emission wavelength were 350 nm and 437 nm .

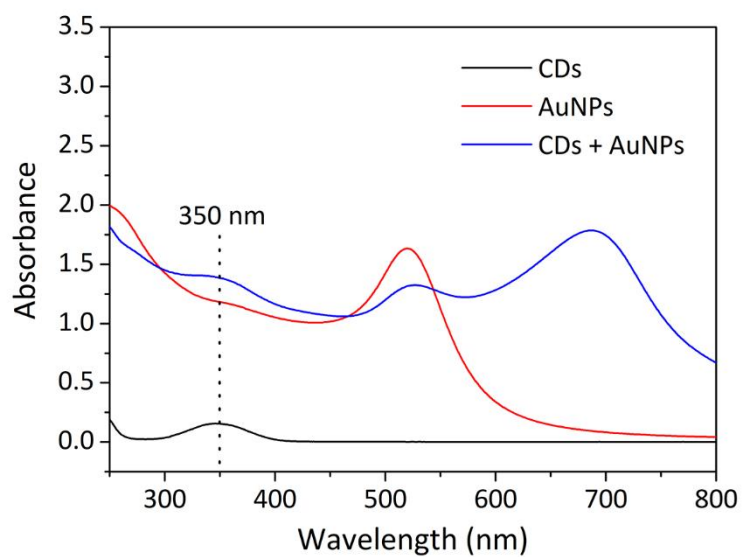


Fig. S4 UV-vis spectra of the prepared CDs in the absence and presence of CC-AuNPs. The concentrations of CDs and CC-AuNPs were $0.2 \mu\text{g}\cdot\text{mL}^{-1}$ and 8 nM, respectively.

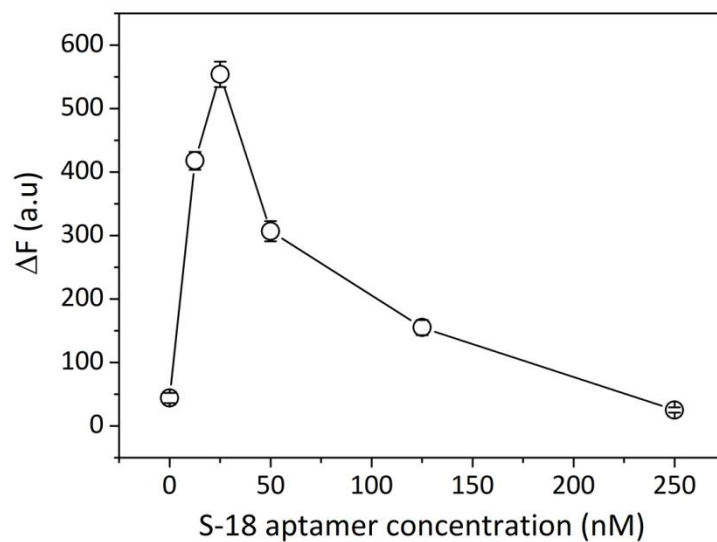


Fig. S5 Effect of S-18 aptamer concentration on the fluorescent aptasensor. The amounts of CDs and CC-AuNPs were $0.2 \text{ mg}\cdot\text{mL}^{-1}$ and 3.2 nM . The excitation and emission wavelength were 350 nm and 437 nm , respectively.

References

1. S.-L. Hu, K.-Y. Niu, J. Sun, J. Yang, N.-Q. Zhao and X.-W. Du, *Journal of Materials Chemistry*, 2009, **19**, 484-488.
2. S. Sahu, B. Behera, T. K. Maiti and S. Mohapatra, *Chemical Communications*, 2012, **48**, 8835-8837.
3. Y. Wu, S. Zhan, L. Wang and P. Zhou, *Analyst*, 2014, **139**, 1550-1561.
4. J. Zheng, H. Zhang, J. Qu, Q. Zhu and X. Chen, *Analytical Methods*, 2013, **5**, 917-924.
5. H.-H. Deng, G.-W. Li, L. Hong, A.-L. Liu, W. Chen, X.-H. Lin and X.-H. Xia, *Food Chemistry*, 2014, **147**, 257-261.
6. B. Meng, Y. Yu, Q. Zhang, S. Wang, D. Hu and K. Zhang, *Biomedical Chromatography*, 2018, **32**.
7. F. Yan, Y. Zou, M. Wang, X. Mu, N. Yang and L. Chen, *Sensors and Actuators B-Chemical*, 2014, **192**, 488-495.
8. R. Wang, Y. Xu, T. Zhang and Y. Jiang, *Analytical Methods*, 2015, **7**, 1701-1706.
9. J. Yang, W. Chen, X. Liu, Y. Zhang and Y. Bai, *Materials Research Bulletin*, 2017, **89**, 26-32.
10. S. Chandra, D. Laha, A. Pramanik, A. R. Chowdhuri, P. Karmakar and S. K. Sahu, *Luminescence : the journal of biological and chemical luminescence*, 2016, **31**, 81-87.
11. P. Weerathunge, R. Ramanathan, R. Shukla, T. K. Sharma and V. Bansal, *Analytical chemistry*, 2014, **86**, 11937-11941.
12. W. Yang, Y. Wu, H. Tao, J. Zhao, H. Chen and S. Qiu, *Analytical Methods*, 2017, **9**, 5484-5493.
13. H. Shi, G. Zhao, M. Liu, L. Fan and T. Cao, *Journal of hazardous materials*, 2013, **260**, 754-761.
14. R. Rapini, A. Cincinelli and G. Marrazza, *Talanta*, 2016, **161**, 15-21.
15. H. Li, Y. Qiao, J. Li, H. Fang, D. Fan and W. Wang, *Biosensors & bioelectronics*, 2016, **77**, 378-384.
16. Y. Qi, F.-R. Xiu, M. Zheng and B. Li, *Biosensors & bioelectronics*, 2016, **83**, 243-249.
17. K. Abnous, N. M. Danesh, M. Ramezani, M. Alibolandi, P. Lavaee and S. M. Taghdisi, *Microchimica Acta*, 2017, **184**, 81-90.
18. J. Guo, Y. Li, L. Wang, J. Xu, Y. Huang, Y. Luo, F. Shen, C. Sun and R. Meng, *Analytical and bioanalytical chemistry*, 2016, **408**, 557-566.
19. N. Sun, Y. Ding, Z. Tao, H. You, X. Hua and M. Wang, *Food Chemistry*, 2018, **257**, 289-294.